Viscous Flow Due to a Permeable Stretching/Shrinking Sheet in a Nanofluid
(Aliran Likat dengan Helaian Meregang/Mengecut dalam Nanobendalir)

NORIHAN MD. ARIFIN, ROSLINDA NAZAR & IOAN POP*

ABSTRACT

The classical problems of forced convection boundary layer flow and heat transfer near the stagnation point on a permeable stretching/shrinking surface in a nanofluid is studied theoretically. The similarity equations were solved numerically for two types of nanoparticles, namely copper and silver in the base fluid of water with the Prandtl number Pr = 6.7850 to investigate the effect of the solid volume fraction or nanoparticle volume fraction parameter φ of the nanofluid. Also the case of conventional or regular fluid (φ = 0) with Pr = 0.7 is considered for comparison with previously known results from the open literature. The comparison showed excellent agreement. The skin friction coefficient, the Nusselt number and the velocity and temperature profiles were presented and discussed in detail. It was found that the nanoparticle volume fraction substantially affects the fluid flow and heat transfer characteristics.

Keywords: Boundary layer; heat transfer; nanofluid; stagnation-point flow; stretching/shrinking sheet

ABSTRAK

Masalah klasik bagi aliran lapisan sempadan olakan paksa dan pemindahan haba berdekatan titik genangan pada permukaan meregang/mengecut yang telap dalam nanobendalir telah dikaji secara teori. Persamaan keserupaan telah diselesaikan secara berangka bagi dua jenis nanozarah, iaitu kuprum dan perak dalam bendalir asas air dengan nombor Prandtl Pr = 6.7850 untuk mengkaji kesan parameter pecahan isipadu pepejal atau pecahan isipadu nanozarah φ bagi nanobendalir. Kes bagi bendalir biasa atau konvensional (φ = 0) dengan Pr = 0.7 dipertimbangkan bagi tujuan perbandingan dengan keputusan terdahulu yang diketahui. Hasil perbandingan tersebut adalah sangat baik. Pekali geseran kulit, nombor Nusselt serta profil-profil halaju dan suhu telah dipersembah dan dibincangkan dengan terperinci. Didapati bahawa pecahan isipadu nanozarah banyak mempengaruhi ciri-ciri aliran bendalir dan pemindahan haba.

Kata kunci: Aliran titik-genangan; helaian meregang/mengecut; lapisan sempadan; nanobendalir; pemindahan haba

INTRODUCTION

Convective heat transfer can be enhanced passively by changing the flow geometry, boundary conditions, or by enhancing thermal conductivity of the fluid. Various techniques have been proposed to enhance the heat transfer performance of fluids. Researchers have also tried to increase the thermal conductivity of base fluids by suspending micro- or larger-sized solid particles in fluids, since the thermal conductivity of solid is typically higher than that of liquid (Table 1) (Wang & Mujumdar 2008a). Numerous theoretical and experimental studies of suspensions containing solid particles have been conducted since Maxwell's theoretical work was published more than 100 years ago (Maxwell 1881). Modern nanotechnology provides new opportunities to process and produce materials with average crystallite sizes below 50 nm. Fluids with nanoparticles suspended in them are called nanofluids, a term first proposed by Choi (1995). Nanofluid is a suspension of nanoparticles in the base fluid. The convective heat transfer characteristic of nanofluids depend on the thermo-physical properties of the base fluid and the ultra fine particles, the flow pattern and flow structure, the volume fraction of the suspended particles, the dimensions and the shape of these particles. Nanofluids are expected to have superior properties compared to conventional heat transfer fluids, as well as fluids containing micro-sized metallic particles. The utility of a particular nanofluid for a heat transfer application can be established by suitably modeling the convective transport in the nanofluid. There are also several numerical and experimental studies on the forced and natural convection using nanofluids related with differentially heated enclosures and we mention here those by Abu-Nada (2008, 2010), Abu-Nada and Oztop (2009), Ghasemi and Aminossadati (2010), Khanafer et al. (2003), Muthtamilselvan et al. (2010), Tiwari and Das (2007), etc. The book by Das et al. (2007) and the recent review papers by Trisaksri and Wongwises (2007), Daungthongsuk and Wongwises (2007), Wang and Mujumdar (2008a, 2008b), and Kakaç and Pramunjaroenkij (2009) present excellent collection of up to now published papers on nanofluids.

However, studies on boundary layer flows in nanofluids are rather limited. Among others are the papers by Nield and Kuznetsov (2009), which deals with the classical problems of natural convective boundary layer

TABLE 1. Thermal conductivities of various solids and liquids (Wang & Mujumdar 2008a)

	Material	Thermal Conductivity (W/m-K)
Metallic solids	copper	401
	aluminum	237
Nonmetallic solids	silicon	148
	alumina (Al_2O_3)	40
Metallic liquids	sodium (644 K)	72.3
Nonmetallic liquids	water	0.613
	ethylene glycol (EG)	0.253
	engine oil (EO)	0.145

flow in a porous medium saturated by a nanofluid, known as the Cheng-Minkowycz's problem; Kuznetsov and Nield (2010) for the problem of natural convective boundary layer flow of a viscous and incompressible fluid past a vertical semi-infinite flat plate with water-based nanofluids; Khan and Pop (2010) and Bachok et al. (2010a) for a stretching flat surface in a nanofluid; Bachok et al. (2010b) for the boundary layer flow past a three-dimensional body embedded in a nanofluid; and Ahmad and Pop (2010) for the mixed convection boundary layer flow past a vertical flat plate embedded in a porous medium filled with nanofluids. We also mention here the very recent papers by Yacob et al. (2011) on the Falkner–Skan problem for a static and moving wedge with prescribed surface heat flux in a nanofluid; Nazar et al. (2011) on the mixed convection boundary layer flow past a horizontal circular cylinder in a nanofluid embedded in a porous medium; and Arifin et al. (2011) on the Marangoni boundary layer flow of a nanofluid.

The aim of the present paper is to extend the classical problem of stagnation-point flow of a viscous and incompressible fluid (Newtonian fluid) on a stretching/shrinking sheet first considered by Wang (2008) to the case of nanofluid using the model of Tiwari and Das (2007). Two different nanoparticles, namely copper and silver are tested to investigate the effects of the nanoparticle volume fraction parameter ϕ of the nanofluid on the flow and heat transfer characteristics. The case of conventional or regular fluid ($\phi = 0$) with the Prandtl number Pr = 0.7 is also considered for comparison with the results reported by Wang (2008). It is found that the comparison shows excellent agreement. It is worth mentioning to this end that the flow over a continuously stretching/shrinking surface is an important problem in many engineering processes with applications in industries such as the hot rolling, wire drawing, and glass-fibre production (Tadmor & Klein 1970). It seems that Miklavčič and Wang (2006) were the first to investigate the flow over a shrinking sheet, which is an exact solution of the Navier-Stokes equations. It was shown that mass suction is required to maintain the flow over a shrinking sheet. Later, there are several other published papers on shrinking surfaces such as those of Hayat et al. (2007), Fang et al. (2008) and Noor and

Hashim (2009), among others. This new type of shrinking sheet flow is essentially a backward flow as discussed by Goldstein (1965) and shows physical phenomena quite distinct from the forward stretching flow.

BASIC EQUATIONS

We consider the steady two-dimensional boundary layer flow near the stagnation-point on a permeable stretching/shrinking sheet in a water based nanofluid containing two types of nanoparticles: copper and silver. The nanofluid is assumed incompressible, the flow is assumed to be laminar and the viscous dissipation and radiation effects are neglected. It is also assumed that the base fluid (i.e. water) and the nanoparticles are in thermal equilibrium and no slip occurs between them. The thermophysical properties of fluid and nanoparticles are given in Table 2 (Abu-Nada & Oztop 2009). Under these assumptions and following the model equations of nanofluid proposed by Tiwari and Das (2007), the basic continuity, momentum and energy equations for the problem under consideration can be written as (Miklavčič & Wang 2006)

$$\frac{\partial u}{\partial x} + \frac{\partial v}{\partial y} = 0. \tag{1}$$

$$u\frac{\partial u}{\partial x} + v\frac{\partial u}{\partial y} + w\frac{\partial u}{\partial z} = u_e\frac{du_e}{dx} + \mu_{nf}\frac{\partial^2 u}{\partial z^2}. \tag{2}$$

$$u\frac{\partial T}{\partial x} + v\frac{\partial T}{\partial y} + w\frac{\partial T}{\partial z} = \alpha_{nf}\frac{\partial^2 T}{\partial z^2}, \tag{3}$$

subject to the boundary conditions:

$$v = 0, \ u = u_w(x) = cx, \ w = w_w, \ T = T_w \ \text{at} \ z = 0$$
$$u = u_e(x) = ax, \ T = T_\infty \ \text{as} \ z \to \infty. \tag{4}$$

Here x, y and z are the Cartesian coordinates with x and y in the plane of the stretching/shrinking sheet ($z = 0$), and the coordinate z being measured normal to the stretching/shrinking sheet, u, v and w are the velocity components along the x, y and z axes, respectively, w_w is the mass flux velocity with $w_w<0$ for suction and $w_w>0$ for injection (blowing), T is the non-dimensional temperature of the nanofluid, T_w is the constant surface temperature

distribution, T_∞ is the uniform temperature of the ambient nanofluid, $u_w(x)$ is the velocity of the stretching/shrinking sheet, $u_e(x)$ is the velocity of the external flow (potential flow) of the nanofluid with c being a constant, with $c > 0$ for a stretching sheet and $c < 0$ for a shrinking sheet, and a is a positive constant. Further, μ_{nf} is the effective viscosity of the nanofluid and α_{nf} is the thermal diffusivity of the nanofluid (Table 2) (Abu-Nada & Oztop 2009), and are defined as:

$$\mu_{nf} = \frac{\mu_f}{(1-\phi)^{2.5}}, \ \alpha_{nf} = \frac{k_{nf}}{(\rho C_p)}, \ \rho_{nf} = (1-\phi)\rho_f + \phi\rho_s,$$

$$(\rho C_p)_{nf} = (1-\phi)(\rho C_p)_f + \phi(\rho C_p)_s, \ \frac{k_{nf}}{k_f} = \frac{k_s + 2k_f - 2\phi(k_f - k_s)}{k_s + 2k_f + \phi(k_f - k_s)},$$

$$(5)$$

where ϕ is the nanoparticle volume fraction, ρ_{nf} is the effective density of the nanofluid, $(\rho C_p)_{nf}$ is the heat capacity of the nanofluid, k_{nf} is the effective thermal conductivity of the nanofluid, ρ_f is the reference density of the fluid fraction, ρ_s is the reference density of the solid fraction, μ_f is the viscosity of the fluid fraction, k_f is the thermal conductivity of the fluid, k_s is the thermal conductivity of the solid, $(\rho C_p)_f$ is the heat capacity of the fluid and $(\rho C_p)_s$ is the heat capacity of the solid.

TABLE 2. Thermophysical properties of fluid and nanoparticles (Abu Nada & Oztop 2009)

Physical properties	Fluid phase (water)	Cu	Ag
C_p (J/kg K)	4179	385	235
ρ (kg/m³)	997.1	8933	10500
k (W/mK)	0.613	400	429

Following Miklavčič and Wang (2006), we look for a similarity solution of Eqs. (1)-(3) subject to the boundary conditions (4) of the following form:

$$u = cxf'(\eta), \ v = -c(m-1)f(\eta), \ \theta(\eta) = (T-T_\infty)/(T_w-T_\infty)$$
$$w = -(av)^{1/2} f(\eta), \ \eta = (a/v)^{1/2}z, \quad (6)$$

where primes denote differentiation with respect to η and $m = 1$ when the sheet shrinks in the x direction only, and $m = 2$ when the sheet shrinks axisymmetrically. Substituting (6) into (2) and (3), the basic equations of this problem can be reduced to the following two uncoupled ordinary differential equations:

$$\frac{1}{(1-\phi)^{2.5}(1-\phi+\phi\rho_s/\rho_f)}f''' + mff'' + 1 - f'^2 = 0. \quad (7)$$

$$\frac{k_{nf}/k_f}{(1-\phi)+\phi(\rho C_p)_s/(\rho C_p)_f}\frac{1}{Pr}\theta'' + mf\theta' = 0, \quad (8)$$

subject to the boundary conditions:

$$f(0) = s, \ f'(0) = \lambda, \ \theta(0) = 1$$
$$f'(\eta) \to 1, \ \theta(\eta) \to 0 \quad \text{as} \quad \eta \to \infty. \quad (9)$$

Here $s = -w_w/(av)^{1/2}$ is the suction ($s > 0$) parameter, $\lambda = c/a$ is the stretching ($\lambda > 0$) or shrinking ($\lambda < 0$) parameter.

The physical quantities of interest are the skin friction coefficient C_f and the local Nusselt number Nu_x. It is easily shown that these quantities are given by:

$$Re_x^{1/2} C_f = \frac{1}{(1-\phi)^{2.5}} f''(0), \ Re_x^{-1/2} Nu_x = -\frac{k_{nf}}{k_f}\theta'(0), \quad (10)$$

where $Re_x = u_e(x)x/v$ is the local Reynolds number.

RESULTS AND DISCUSSION

The nonlinear ordinary differential equations (7) and (8) subject to the boundary conditions (9) are solved numerically using the shooting method. This well-known technique is an iterative algorithm which attempts to identify appropriate initial conditions for a related initial value problem (IVP) that provides the solution to the original boundary value problem (BVP). The shooting method is based on MAPLE "dsolve" command and MAPLE implementation, "shoot" (Meade et al. 1996). Following Khanafer et al. (2003), Tiwari and Das (2007) and Abu-Nada and Oztop (2009), we have considered the range of nanoparticle volume fraction as $0 \le \phi \le 0.2$. The Prandtl number Pr of the base fluid (water) is kept constant at 6.7850. Further, it should also be pointed out that the thermophysical properties of fluid and nanoparticles (Cu, Ag) used in this study are given in Table 2. On the other hand, it is worth mentioning that, the present study reduces to regular Newtonian fluid when $\phi = 0$. Therefore, in order to validate the present numerical method used, we have compared our results with those obtained by Wang (2008) for different values of the stretching/shrinking parameter λ when $\phi = 0$ (regular Newtonian fluid) for $m = 1$ (when the sheet shrinks in the x direction only) and $m = 2$ (when the sheet shrinks axisymmetrically), respectively. The comparisons are found to be in very good agreement (Table 3 & 4). Therefore, the present numerical solution is further validated, so that we are confident the present results are accurate.

On the other hand, the values of $f''(0)$ for Cu nanoparticles with $\phi \neq 0$, namely $\phi = 0.1$ and $\phi = 0.2$ are also included in Table 3. Variation of the skin friction coefficient $Re_x^{1/2} C_f$ with λ for different types of nanoparticles (Cu, Ag) when $m = 1$ (when the sheet shrinks in the x direction only), $\phi = 0.1$ and $s = 0$ (impermeable surface) are shown in Figure 1. It is seen that there are regions of unique solutions for $\lambda > -1$, dual solutions for $\lambda_c < \lambda \le -1$ and no solutions for $\lambda < \lambda_c$, where λ_c is the critical value of λ. Based on our computation, $\lambda_c = -1.2465$ for $\phi = 0$ and $\lambda_c = -1.24658$ for $\phi \neq 0$. It is observed from Figure 1 that for $\lambda > 1$ the values of the skin friction coefficient $Re_x^{1/2} C_f$ are slightly higher for

TABLE 3. Values of $f''(0)$ for Cu nanoparticles with $m = 1$ and $s = 0$ (impermeable surface)

	Wang (2008) $f''(0)$		Present $f''(0)$	
λ	$\phi = 0$	$\phi = 0$	$\phi = 0.1$	$\phi = 0.2$
1	0	0	0	0
0.5	0.71330	0.71330	0.8379	0.8688
0.2	1.05113	1.05113	1.2348	1.2803
0.1	1.14656	1.14656	1.3469	1.3966
0	1.232588	1.232588	1.4480	1.5013
-0.25	1.40224	1.40224	1.6473	1.7080
-0.5	1.49567	1.49567	1.7570	1.8218
-0.75	1.48930	1.48930	1.7495	1.8140
-1	1.32882	1.32882	1.5610	1.6186
-1.15	1.08223	1.08223	1.2713	1.3182
	(0.116702)	(0.116702)	(0.1371)	(0.1421)
-1.2465	0.55430	0.55430	0.6864	0.7117
			(0.6511)	(0.6751)
-1.24658			0.6682	0.6934

Results in parenthesis ( ) are the second (dual) solutions

TABLE 4. Values of $f''(0)$ for $\phi = 0$ with $m = 2$ and $s = 0$ (impermeable surface)

λ	Wang (2008) $f''(0)$	Present $f''(0)$
1	0	0
0.5	0.78032	0.78032
0.2	1.13374	1.13374
0.1	1.22911	1.22911
0	1.311938	1.311938
-0.25	1.45664	1.45664
-0.5	1.49001	1.49001
-0.75	1.35284	1.35284
-0.95	0.94690	0.94690
-0.9945	0.5	0.64502
-0.99945		0.500204
-1	0	0.319476

FIGURE 1. Variation of the skin friction coefficient $Re_x^{1/2} C_f$ with λ for different types of nanoparticles when $m = 1$, $\phi = 0.1$ and $s = 0$

nanoparticles Cu compared to Ag, while for $\lambda < 1$, the opposite behaviour is observed. It is also shown that the values of $Re_x^{1/2} C_f$ are higher for the shrinking sheet ($\lambda < 0$) compared to the stretching sheet ($\lambda > 0$). It is worth mentioning that all the entire values of the skin friction coefficient are positive for $\lambda < 1$, while they are negative when $\lambda > 1$. Physically, the negative sign of the skin friction coefficient corresponds to the surface exerts a drag force on the fluid and the positive sign implies the opposite. On the other hand, the skin friction coefficient is zero when $\lambda = 1$ regardless of the values of other parameters. This is not surprising since there is no shear stress at the surface when the surface and the fluid move
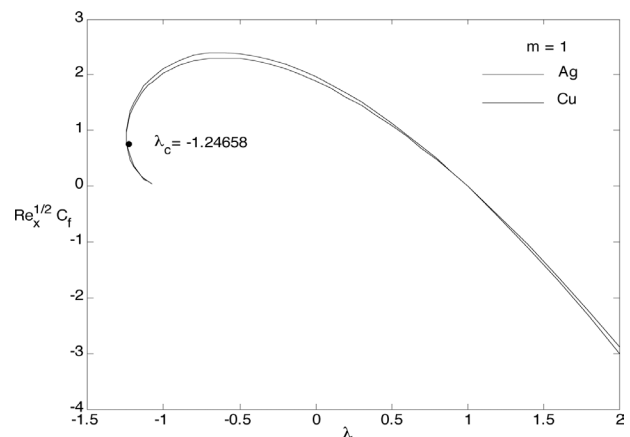
with the same velocity (Weidman et al. 2006; Yacob et al. 2011). However, the heat transfer between the fluid and the surface still occurs for this case (Figure 2) since they are at different temperatures.

Figure 2 shows the corresponding variation of the local Nusselt number $Re_x^{-1/2} Nu_x$ with λ for different types of nanoparticles (Cu, Ag) when $m = 1$, $\phi = 0.1$ and $s = 0$. It is seen that there are also regions of unique solutions for $\lambda > -1$, dual solutions for $\lambda_c < \lambda \leq -1$ and no solutions for $\lambda < \lambda_c$, where λ_c is the critical value of λ. It is shown that as λ decreases, the local Nusselt number also decreases. On the other hand, variation of the skin friction coefficient $Re_x^{1/2} C_f$ and the local Nusselt number $Re_x^{-1/2} Nu_x$ with λ for Cu nanoparticles when $m = 1$, $\phi = 0.1$ and several values of s are shown in Figures 3 and 4,
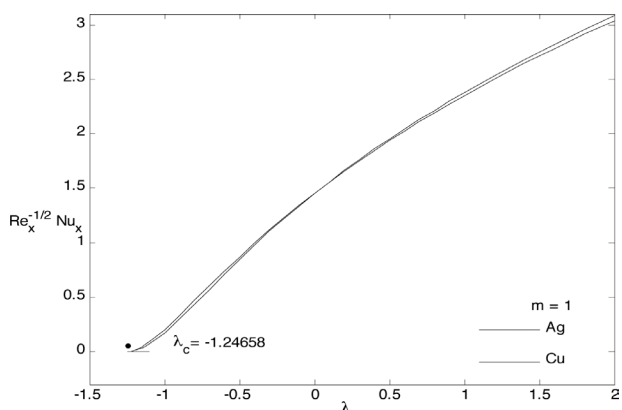
respectively. It is shown in Figure 3 that for $\lambda < 1$, as the suction parameter s increases (the suction is stronger), the skin friction coefficient increases and the points beyond which no solutions exist also increases, thus we can say that suction delays the separation of boundary layer. On the other hand, it is seen from Figure 4 that for all values of λ, as the suction parameter s increases, the local Nusselt number also increases, and as λ decreases, the local Nusselt number also decreases, and it is seen again that suction delays separation.

The values of $f''(0)$ for $\phi = 0$ (regular Newtonian fluid) with $m = 2$ (when the sheet shrinks axisymmetrically) and $s = 0$ (impermeable surface) are shown in Table 4, while the values of $f''(0)$ and $-\theta'(0)$ for Cu nanoparticles with $m = 2$ and $s = 0.5$ are presented in Tables 5 and 6, respectively. Based on our computation, the solutions are not unique for $s \geq 0.407$. Variation of the skin friction coefficient $\mathrm{Re}_x^{1/2} C_f$ and the local Nusselt number $\mathrm{Re}_x^{-1/2} Nu_x$ with λ for Cu nanoparticles when $m = 2$, $\phi = 0.1$ and several values of s are shown in Figures 5 and 6, respectively. It is again

FIGURE 4. Variation of the local Nusselt number $\mathrm{Re}_x^{-1/2} Nu_x$ with λ for Cu nanoparticles when $m = 1$, $\phi = 0.1$ and various values of s

FIGURE 2. Variation of the local Nusselt number $\mathrm{Re}_x^{-1/2} Nu_x$ with λ for different types of nanoparticles when $m = 1$, $\phi = 0.1$ and $s = 0$
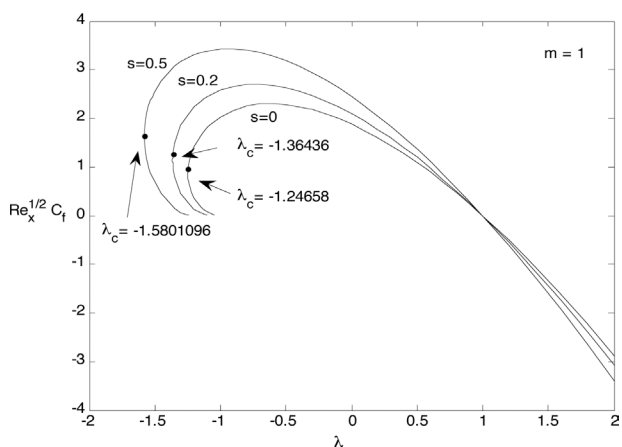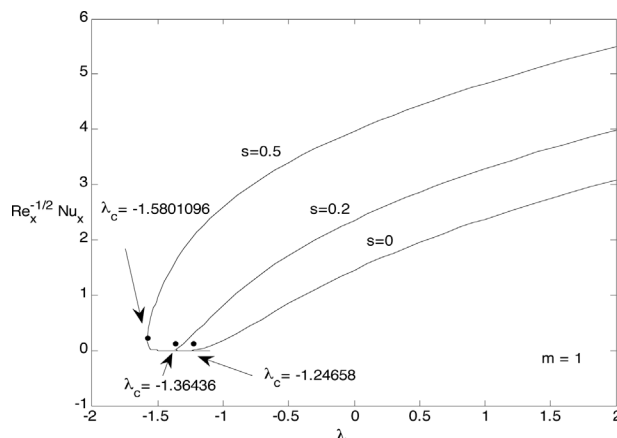

FIGURE 3. Variation of the skin friction coefficient $\mathrm{Re}_x^{1/2} C_f$ with λ for Cu nanoparticles when $m = 1$, $\phi = 0.1$ and various values of s

TABLE 5. Values of $f''(0)$ for Cu nanoparticles with $m = 2$ and $s = 0.5$

	$f''(0)$		
λ	$\phi = 0$	$\phi = 0.1$	$\phi = 0.2$
1	0	0	0
0.5	1.1031	1.3690	1.4386
0.2	1.6614	2.0716	2.1792
0.1	1.8279	2.2835	2.4031
0	1.9839	2.4833	2.6146
-0.25	2.3229	2.9255	3.0846
-0.5	2.5785	3.2747	3.4593
-0.75	2.7298	3.5102	3.7182
-1	2.7373	3.5954	3.8255
-1.2	2.6361	3.5042	3.7535
	(0.4403)	(0.44002)	(0.44000)
-1.25	1.08223	3.4483	3.7036
	(0.5672)	(0.5634)	(0.5631)
-1.3	2.3858	3.3736	3.6360
	(0.7150)	(0.6974)	(0.6955)
-1.4	1.9819	3.1422	3.4276
	(1.1912)	(1.0368)	(1.0219)
-1.425	1.6396	3.0579	3.3533
	(1.5514)	(1.1475)	(1.1250)
-1.42530704	1.5956		
-1.50		2.6510	3.0267
		(1.6343)	(1.5385)
-1.525		2.2882	2.8448
		(2.0240)	(1.7498)
-1.526762		2.1570	
-1.55			2.4939
			(2.1301)
-1.553			2.3288
			(2.2989)
-1.553020			2.3120

Results in parenthesis ( ) are the second (dual) solutions

TABLE 6. Values of $-\theta'(0)$ for Cu nanoparticles
with $m = 2$ and $s = 0.5$

		$-\theta'(0)$	
λ	$\phi = 0$	$\phi = 0.1$	$\phi = 0.2$
1	8.2292	6.3563	5.0079
0.5	7.7302	5.9489	4.6678
0.2	7.3919	5.6749	4.4400
0.1	7.2705	5.5772	4.3588
0	7.1440	5.4757	4.2748
-0.25	6.8003	5.2024	4.0493
-0.5	6.4033	4.8927	3.7956
-0.75	5.9206	4.5291	3.5013
-1	5.2713	4.0749	3.1416
-1.2	4.4418 (3×10^{-19})	3.5846 (4×10^{-15})	2.7680 (0)
-1.25	4.1225 (1×10^{-11})	3.4291 (0.0000001)	2.6538 (0.0000002)
-1.3	3.6982 (0.0000003)	3.2516 (0.00002)	2.5267 (0.00005)
-1.4	1.8903 (0.0065)	2.7862 (0.0029)	2.2127 (0.0097)
-1.425	0.4647 (0.2604)	2.6296 (0.0101)	2.1144 (0.0230)
-1.42530704	0.3524		
-1.50		1.8875 (0.2266)	1.7165 (0.1848)
-1.525		1.2137 (0.7456)	1.5062 (0.8912)
-1.526762		0.9740	
-1.55			1.1083 (0.7087)
-1.553			0.9241 (0.8912)
-1.553020			0.9056

Results in parenthesis ( ) are the second (dual) solutions

FIGURE 5. Variation of the skin friction coefficient $\mathrm{Re}_x^{1/2} C_f$ with λ for Cu nanoparticles when $m = 2$, $\phi = 0.1$ and various values of s
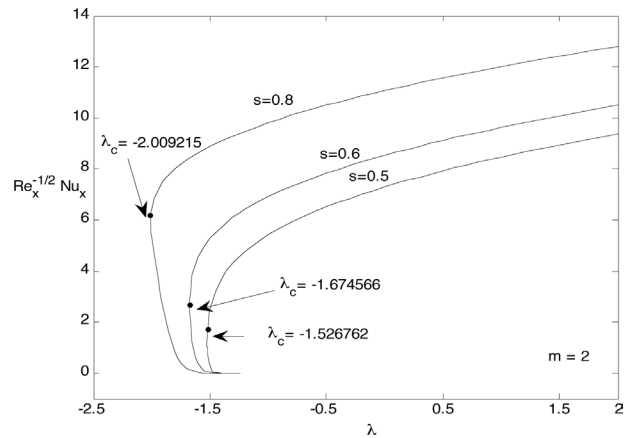
FIGURE 6, Variation of the local Nusselt number $\mathrm{Re}_x^{-1/2} Nu_x$ with λ for Cu nanoparticles when $m = 2$, $\phi = 0.1$ and various values of s

TABLE 7. Values of λ_c, $f''(0)$ and $-\theta'(0)$ for Cu nanoparticles

m	s	λ_c	$f''(0)$	$-\theta'(0)$
1	0	-1.24658	0.6682	0.0001
	0.2	-1.36436	0.8796	0.0033
	0.5	-1.5801096	1.2603	0.1362
2	0.5	-1.526762	2.1568	0.9764
	0.6	-1.674566	2.5850	1.9856
	0.8	-2.009215	3.6230	4.4621

seen in these figures that suction delays separation of boundary layer, i.e. as the value of the suction parameter increases, the critical point $|\lambda_c|$ increases. It is also seen that in the case of $m = 2$, there are regions of unique solutions for $\lambda > -1$, dual solutions for $\lambda_c < \lambda \le -1$ and no solutions for $\lambda < \lambda_c$, where λ_c is the critical value of λ as presented in Table 7. As in similar physical situations, from Figures 1 to 6, we postulate that the upper branch solutions are physically stable and occur in practice, whilst the lower branch solutions are not physically realizable. This postulate can be verified by performing a stability analysis but this is beyond the scope of the present paper. However, such an analysis has been done in the papers by Harris et al. (2009), Merkin (1985) and Weidman et al. (2006).
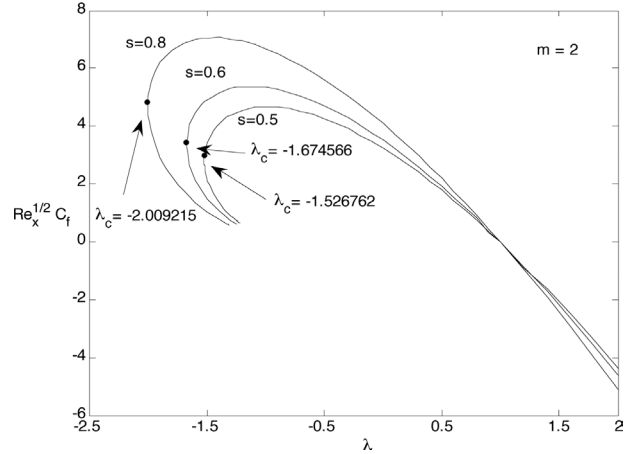
Figures 7 and 8 display the velocity and temperature profiles for different types of nanoparticles (Cu, Ag) when $m = 1$ (when the sheet shrinks in the x direction only), $\phi = 0.1$, $\lambda = -1.2$ and $s = 0$ (impermeable surface). Figures 9 and 10 show the velocity and temperature profiles for different types of nanoparticles (Cu, Ag) when $m = 2$ (when the sheet shrinks axisymmetrically), $\phi = 0.1$, $\lambda = -1.5$ and $s = 0.5$ (permeable surface). The
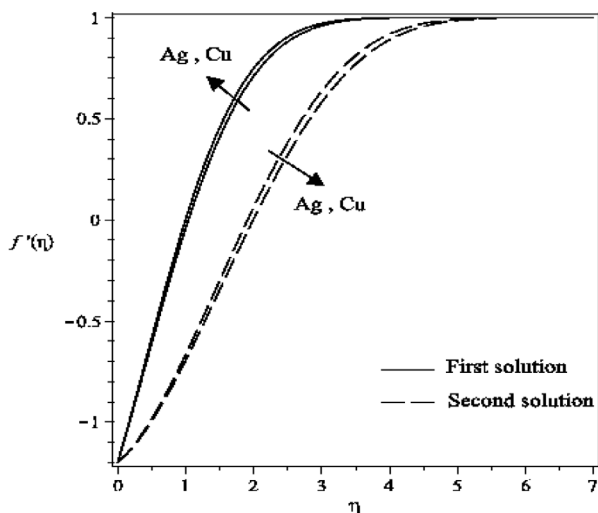
FIGURE 7. Velocity profiles $f'(\eta)$ for different types of nanoparticles when $m = 1$, $\phi = 0.1$, $\lambda = -1.2$ and $s = 0$
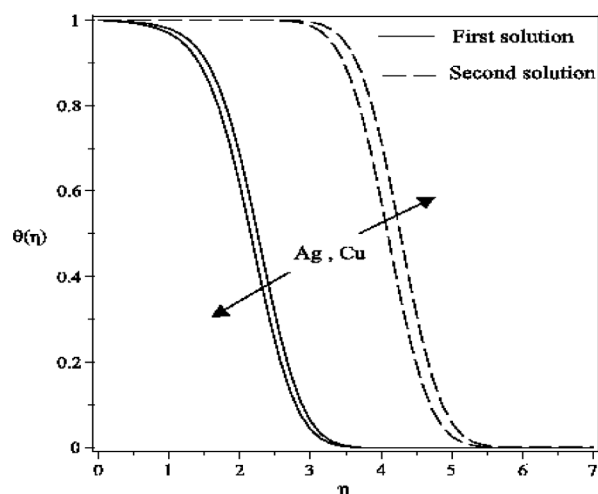

FIGURE 9. Velocity profiles $f'(\eta)$ for different types of nanoparticles when $m = 2$, $\phi = 0.1$, $\lambda = -1.5$ and $s = 0.5$

FIGURE 8. Temperature profiles $\theta(\eta)$ for different types of nanoparticles when $m = 1$, $\phi = 0.1$, $\lambda = -1.2$ and $s = 0$

FIGURE 10. Temperature profiles $\theta(\eta)$ for different types of nanoparticles when $m = 2$, $\phi = 0.1$, $\lambda = -1.5$ and $s = 0.5$

velocity and temperature profiles for first (upper branch) and second (lower branch) solutions are presented in these figures. The second (lower branch) solution profiles prove the existence of dual solutions. It is shown in Figures 8 and 10 that the heat transfer rate at the surface is higher for nanoparticles Cu than Ag. Figures 11 and 12 show the velocity and temperature profiles for Cu nanoparticles when $\phi = 0.1$, $m = 1$, $\phi = -1.5$, and various value of s, respectively, while Figures 13 and 14 illustrate the velocity and temperature profiles for Cu nanoparticles when $\phi = 0.1$, $m = 2$, $\lambda = -1.5$, and various value of s, respectively. It is seen in Figures 11 and 13 that the velocity gradient on the surface increases as s increases and this is consistent with the results obtained for the skin friction coefficient in Figures 3 and 5. Finally, it is worth mentioning that all the velocity and temperature profiles presented in
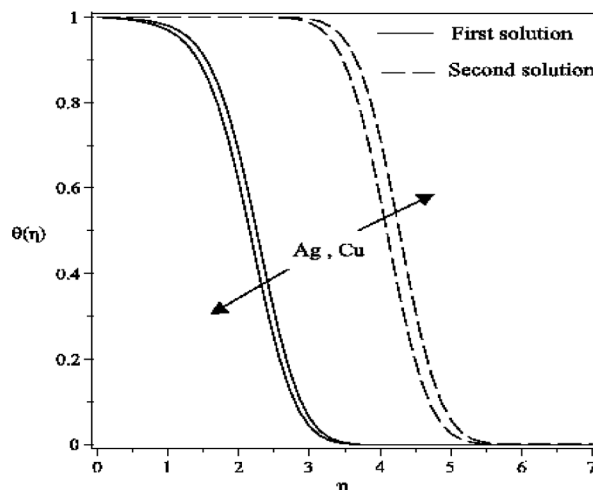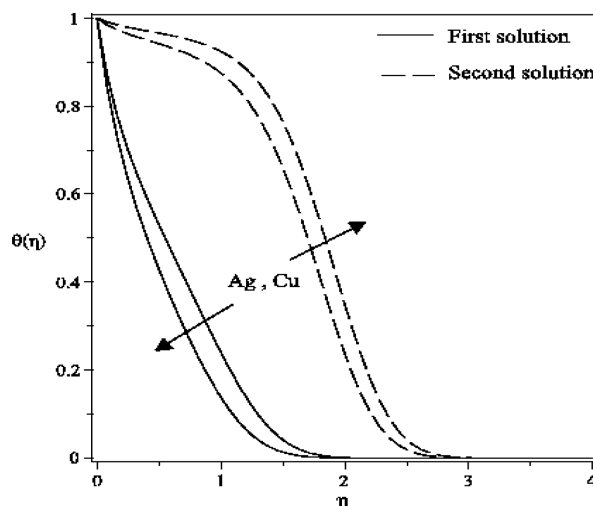
Figures 7 to 14 satisfy the far field boundary conditions (9) asymptotically and thus, support the validity of the dual solutions obtained.

CONCLUSION

The problem of forced convection boundary layer flow and heat transfer near the stagnation point on a permeable stretching/shrinking surface in a nanofluid is studied theoretically. The similarity equations are solved numerically for two types of nanoparticles, namely copper and silver in the base fluid of water with the Prandtl number Pr = 6.7850, to investigate the effect of the nanoparticle volume fraction parameter ϕ. Results for the skin friction coefficient, local Nusselt number as well as the velocity and temperature profiles are presented for different values of the governing parameters.
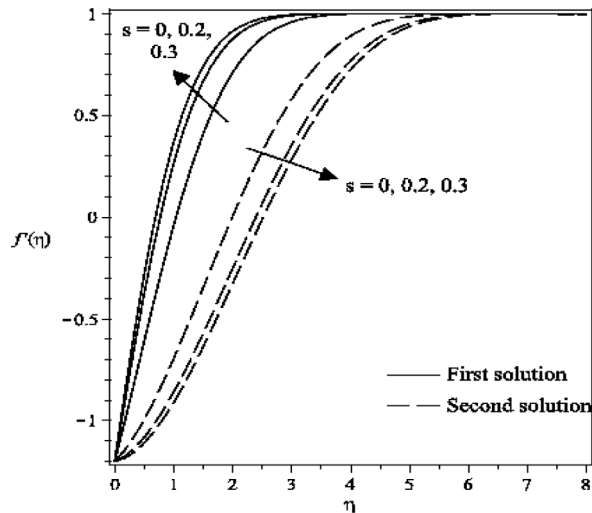
1366

FIGURE 11. Velocity profiles $f'(\eta)$ for Cu nanoparticles when
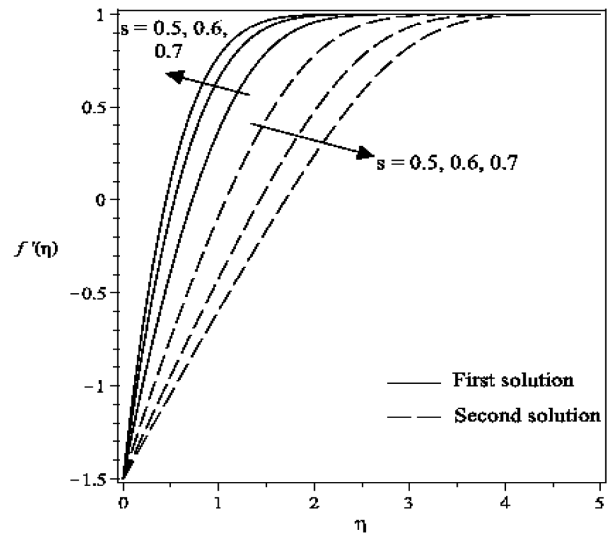$m = 1$, $\phi = 0.1$, $\lambda = -1.2$ and various values of s

FIGURE 13. Velocity profiles $f'(\eta)$ for Cu nanoparticles when
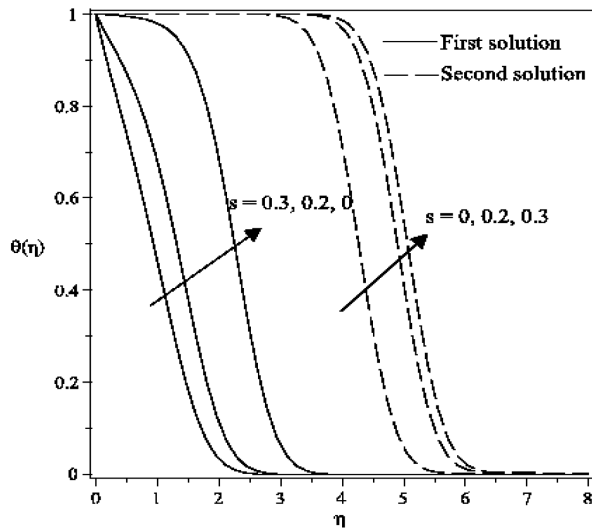$m = 2$, $\phi = 0.1$, $\lambda = -1.5$ and various values of s

FIGURE 12. Temperature profiles $\theta(\eta)$ for Cu nanoparticles
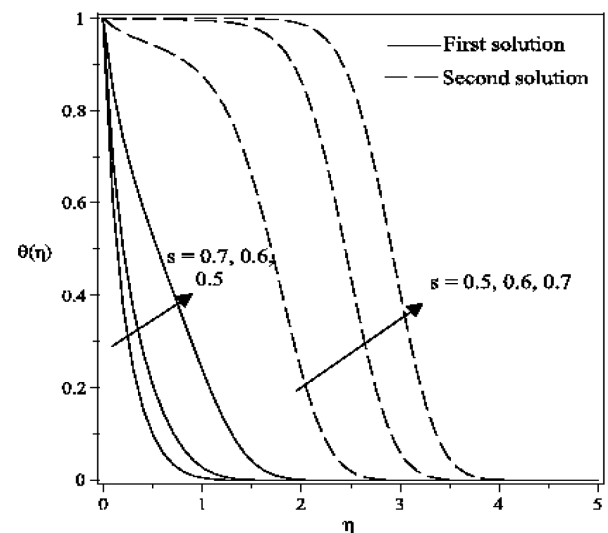when $m = 1$. $\phi = 0.1$, $\lambda = -1.2$ and various values of s

FIGURE 14. Temperature profiles $\theta(\eta)$ for Cu nanoparticles
when $m = 2$, $\phi = 0.1$, $\lambda = -1.5$ and various values of s

REFERENCES

Abu-Nada, E. 2010. Effects of variable viscosity and thermal conductivity of CuO-water nanofluid on heat transfer enhancement in natural convection: mathematical model and simulation. *ASME J. Heat Transfer* 132: 052401-1 – 052401-9.

Abu-Nada, E. 2008. Application of nanofluids for heat transfer enhancement of separated flows encountered in a backward facing step. *Int. J. Heat Fluid Flow* 29: 242-249.

Abu-Nada, E. & Oztop, H.F. 2009. Effects of inclination angle on natural convection in enclosures filled with Cu-water nanofluid. *Int. J. Heat Fluid Flow* 30: 669-678.

Ahmad, S. & Pop, I. 2010. Mixed convection boundary layer flow from a vertical flat plate embedded in a porous medium filled with nanofluids. *Int. Comm. Heat Mass Transfer* 37: 987-991.

Arifin, N.M., Nazar, R. & Pop, I. 2011. Non-isobaric Marangoni boundary layer flow for Cu, Al$_2$O$_3$ and TiO$_2$ nanoparticles in a water based fluid. *Meccanica* 46: 833-843.

Bachok, N., Ishak, A. & Pop, I. 2010a. Boundary-layer flow of nanofluids over a moving surface in a flowing fluid. *Int. J. Thermal Sci.* 49: 1663-1668.

Bachok, N., Ishak, A., Nazar, R. & Pop, I. 2010b. Flow and heat transfer at a general three-dimensional stagnation point in a nanofluid. *Physica B* 405: 4914-4918.

Choi, S.U.S. 1995. Enhancing thermal conductivity of fluids with nanoparticles. In *Development and Applications of non-Newtonian Flows*, edited by D.A. Siginer & H.P. Wan. ASME MD-vol. 231 and FED-vol. 66.

Das, S.K., Choi, S.U.S., Yu, W. & Pradet, T. 2007. *Nanofluids: Science and Technology*. New Jersey: Wiley.

Daungthongsuk, W. & Wongwises, S. 2007. A critical review of convective heat transfer nanofluids. *Renew. Sust. Eng. Rev.* 11: 797-817.

Fang, T., Liang, W. & Lee, C.F. 2008. A new solution branch for the Blasius equation – a shrinking sheet problem. *Comput. Math. Appl.* 56: 3088-3095.

Ghasemi, B. & Aminossadati, S.M. 2010. Mixed convection in a lid-driven triangular enclosure filled with nanofluids. *Int. Comm. Heat Mass Transfer* 37: 1142-1148.

Goldstein, S. 1965. On backward boundary layers and flow in converging passages. *J. Fluid Mech.* 21: 33-45.

Harris, S.D., Ingham, D.B. & Pop, I. 2009. Mixed convection boundary-layer flow near the stagnation point on a vertical surface in a porous medium: Brinkman model with slip. *Trans. Porous Media* 77: 267-285.

Hayat, T., Abbas, Z. & Sajid, M. 2007. On the analytic solution of magnetohydrodynamic flow of a second grade fluid over a shrinking sheet. *ASME J. Appl. Mech.* 74: 1165-1171.

Kakaç , S. & Pramuanjaroenkij, A. 2009. Review of convective heat transfer enhancement with nanofluids. *Int. J. Heat Mass Transfer* 52: 3187-3196.

Khanafer, K., Vafai, K. & Lightstone, M. 2003. Buoyancy-driven heat transfer enhancement in a two-dimensional enclosure utilizing nanofluids. *Int. J. Heat Mass Transfer* 46: 3639-3653.

Khan, W. A. & Pop, I. 2010. Boundary-layer flow of a nanofluid past a stretching sheet. *Int. J. Heat Mass Transfer* 53: 2477-2483.

Kuznetsov, A.V. & Nield, D.A. 2010. Natural convective boundary-layer flow of a nanofluid past a vertical plate. *Int. J. Thermal Sci.* 49: 243-247.

Maxwell, J.C. 1881. *A Treatise on Electricity and Magnetism 2nd edition*. Oxford: Clarendon Press.

Meade, D.B., Haran, B.S. & White, R.E. 1996. The shooting technique for the solution of two-point boundary value problems. *Maple Tech.* 3: 85-93.

Merkin, J.H. 1985. On dual solutions occurring in mixed convection in a porous medium. *J. Engng. Math.* 20: 171-179.

Miklavčič, M. & Wang, C.Y. 2006. Viscous flow due to a shrinking sheet. *Quart. Appl. Math.* 46: 283-290.

Muthtamilselvan, M., Kandaswamy, P. & Lee, J. 2010. Heat transfer enhancement of copper-water nanofluids in a lid-driven enclosure. *Comm. Nonlinear Sci. Numer. Simul.* 15: 1501-1510.

Nazar, R., Tham, L. Pop, I. & Ingham, D.B. 2011. Mixed convection boundary layer flow from a horizontal circular cylinder embedded in a porous medium filled with a nanofluid. *Trans. Porous Media* 86: 547-566.

Nield, D.A. & Kuznetsov, A.V. 2009. The Cheng–Minkowycz problem for natural convective boundary-layer flow in a porous medium saturated by a nanofluid. *Int. J. Heat Mass Transfer* 52: 5792-5795.

Noor, N.F.M. & Hashim, I. 2009. MHD flow and heat transfer adjacent to a shrinking sheet embedded in a porous medium. *Sains Malaysiana* 38: 559-565.

Tadmor, Z. & Klein, I. 1970. *Engineering Principles of Plasticating Extrusion. Polymer Science and Engineering Series,* New York:Van Norstrand Reinhold.

Tiwari, R.K. & Das, M.K. 2007. Heat transfer augmentation in a two-sided lid-driven differentially heated square cavity utilizing nanofluids, *Int. J. Heat Mass Transfer* 50: 2002-2018.

Trisaksri, V. & Wongwises, S. 2007. Critical review of heat transfer characteristics of nanofluids. *Renew. Sustain. Energy Rev.* 11: 512-523.

Wang, C.Y. 2008. Stagnation flow towards a shrinking sheet. *Int. J. Non-Linear Mech.* 43: 377-382.

Wang, X.-Q. & Mujumdar, A.S. 2008a. A review of nanofluids – Part I: theoretical and numerical investigations. *Brazilian J. Chemical Engng.* 25: 613-630.

Wang, X.-Q. & Mujumdar, A.S. 2008b. A review on nanofluids – Part II: Eexperimental and applications. *Brazilian J. Chemical Engng.* 25: 631-648.

Weidman, P.D., Kubitschek, D.G. & Davis, A.M.J. 2006. The effect of transpiration on self-similar boundary layer flow over moving surface. *Int. J. Engng. Sci.* 44: 730-737.

Yacob, N.A., Ishak, A., Nazar, R. & Pop, I. 2011. Falkner-Skan problem for a static and moving wedge with prescribed surface heat flux in a nanofluid. *Int. Comm. Heat Mass Transfer* 38: 149-153.

Norihan Md. Arifin
Department of Mathematics and Institute for Mathematical Research
Universiti Putra Malaysia
43400 UPM Serdang, Selangor D.E.
Malaysia

Roslinda Nazar
School of Mathematical Sciences
Faculty of Science & Technology & Solar Energy Research Institute
Universiti Kebangsaan Malaysia
43600 UKM Bangi, Selangor D.E.
Malaysia

Ioan Pop*
Faculty of Mathematics
University of Cluj
R-3400 Cluj, CP 253
Romania

*Corresponding author; email: popm.ioan@yahoo.co.uk